

Oct. 5-9, 2010
MONTRÉAL, QUÉBEC, CANADA

MWP 2010

2010 IEEE International Topical Meeting on microwave photonics

Proceedings
2010 IEEE International Topical Meeting on microwave
photonics



Technically supported by



IEEE Catalog Number: CFP10756-PRT
ISBN: 978-1-4244-7822-4

WE3-5 14:45-15:00	
A Dispersion-Insensitive UWB over Fiber System Based on a Photonic Microwave Bandpass Filter	54
<i>S. Pan, J. Yao</i>	
WE3-6 15:00-15:15	
Consolidation of Signal Processing Functions in WDM-Based mm-Wave Fiber Wireless Links using a LCoS-Based Programmable Optical Processor	58
<i>C. Lim, C. Pulikkaseril, K. Lee, A. Nirmalathas, M. Roelens</i>	
WE3-7 15:15-15:30	
Non-Linear Distortions in Electro-Optical Phase Modulators	62
<i>R. Tavlykaev and G. Gopalakrishnan</i>	

Session WE4: Poster Session I – Microwave Photonics Devices and Systems

16:00-17:30 Fontaine GH

Session Co-Chairs:

Arye Rosen, Drexel University, United States

Asher Madjar, M2 Microwaves LLC, United States

WE4-2

Bidirectional Transmission of Digital Signals in a WDM-PolMUX Optical Access Network	66
<i>F. Grassi, J. Mora, B. Ortega</i>	

WE4-3

Performance Evaluation of MB-OFDM Ultra-Wideband over Fiber Transmission Using a Low Cost Electro-Absorption Modulator Integrated Laser.....	70
<i>C. Sui, B. Hraimel, X. Zhang, K. Wu, B. Hraimel, T. Liu, T. Xu, Q. Nie</i>	

WE4-5

Optical Distribution of Microwave Signals for Earth Observation Satellites	74
<i>R. Palacio, F. Deborgies, P. Piironen</i>	

WE4-6

High Power Microwave Pulse Impact on an All-Dielectric Lithium Niobate Modulator	78
<i>J. H. Schaffner, K. Geary, D. Yap, O. Efimov, D. A. White, M. L. Stowell, C. G. Brown, J. S. Levine</i>	

WE4-7

Broadband Microwave and mm-Wave Dispersion Using Periodic Structures	82
<i>J. D. Schwartz, Q. Zhuge, Y. Zhu, J. Azaña, D. V. Plant</i>	

WE4-9

Behavioral Modeling of Radio-over-Fiber Links Using Memory Polynomials.....	85
<i>L. C. Vieira, N. J. Gomes, A. Nkansah, F. van Dijk</i>	

WE4-10	
Equivalent $\lambda/4$ Phase Shift to Improve the Single Longitudinal Mode Property of Asymmetric Sampled Bragg Grating Semiconductor Laser	89
<i>Y. Zhou, Y. Shi, S. Li, J. Li, X. Chen</i>	
WE4-11	
Mitigation of RF Power Degradation in Dispersion-Based Photonic True Time Delay Systems	93
<i>X. Xue, X. Zheng, H. Zhang, B. Zhou</i>	
WE4-12	
Performance Characterization and Limitation of Coherence Multiplexing Technique in Radio over Fiber Systems.....	96
<i>Y. Pei, B. Hraimel, Y. Shen, X. Zhang, K. Xu, X. Sun, J. Wu, J. Lin</i>	
WE4-13	
Experimental Evaluation of High Speed Impulse Radio UWB Interference on WiMAX Narrowband Systems.....	100
<i>X. Yu, X. Yin, I. Tafur Monroy</i>	
WE4-14	
Timing Jitter Reduction of a Mode-Locked VECSEL Using an Optically Triggered SESAM.....	103
<i>G. Baili, L. Morvan, M. Alouini, D. Dolfi, A. Khadour, S. Bouchoule, J. Oudar</i>	
WE4-15	
Integration of Traveling-Wave Photodetector and Coplanar-Fed Log-Periodic Antenna for Terahertz Generation	107
<i>E. Mortazy, K. Wu, H. Liu</i>	
WE4-16	
High Linearity Photodiode Array with Monolithically Integrated Wilkinson Power Combiner....	111
<i>Y. Fu, H. Pan, Z. Li, J. C. Campbell</i>	
WE4-17	
Eliminating Gain Transience in RoF Signals in Dynamic WDM Networks Using a Transient-Suppressed-EDFA with Additional Gain-Stabilization	114
<i>Y. Awaji, T. Kawanishi, B. J. Puttnam, K. Inagaki, N. Wada</i>	
WE4-18	
Frequency Dependence in RF Gain Resonance by Negative Photocurrent Resistance of Electroabsorption Modulator	118
<i>D. Shin, Hanyang University, Republic of Korea</i>	
WE4-19	
Quasi-static Approach to Optimize RF Modulation of Vertical-Cavity Surface-Emitting Lasers	121
<i>Z. Bouhamri, Y. Le Guennec, J. Duchamp, G. Maury, B. Cabon</i>	

WE4-20

- Novel Fiber RF Antenna with Coaxial Structure** 125
X. Shi, S. Zheng, H. Chi, X. Jin, X. Zhang

WE4-21

- 4 Channels Subcarrier Multiplexing Optical Link Using an RSOA Modulator** 128
Zhansheng Liu, Manuel Violas and Mojtaba Sadeghi

WE4-22

- Design and Realization of an Integrated Optical Frequency Modulation Discriminator for a High Performance Microwave Photonic Link** 131
D. Marpaung, C. Roeloffzen, R. Timens, A. Leinse, M. Hoekman

WE4-23

- Electromagnetic Modeling of SPP Resonance for Low Noise RF Magnitude Modulation of Optical Carriers** 135
C. Tripon-Canseliet, S. Faci

WE4-24

- 60GHz CMOS-APD Optoelectronic Mixers with Optimized Conversion Efficiency.....** 139
J. Kim, M. Lee, W. Choi

WE4-25

- Calibration Method of Optoelectronic Frequency Response Using Mach-Zehnder Modulator** 143
K. Inagaki, T. Kawanishi

Session TH1: Photonic Generation of Microwave and THz Signals

8:00-10:00 Verdun/Lachine/Lasalle Ballroom

Session Co-Chairs:

*Alwyn Seeds, University College London, United Kingdom
Idelfonso Tafur Monroy, DTU Fotonik, Denmark*

TH1-1 8:00-8:30

- Application of THz Sensing to Analysis of Works of Art for Conservation (Invited)** 147
K. Fukunaga, I. Hosako, M. Picollo, Y. Kohdzuma

TH1-2 8:30-8:45

- A Compact Tunable Coherent Terahertz Source Based on an Hybrid Integrated Optical Phase-lock Loop** 151
L. Ponnampalam, R. J. Steed, M. J. Fice, C. C. Renaud, D. C. Rogers, D. G. Moodie, G. D. Maxwell, I. F. Lealman, M. J. Robertson, L. Pavlovic, L. Naglic, M. Vidmar, A. J. Seeds

TH1-3 8:45-9:00

- Phase Noise Measurements of a Dual-Wavelength Brillouin Fiber Laser (Student Paper Finalist)** 155
P. T. Callahan, M. C. Gross, M. L. Dennis

60GHz CMOS-APD Optoelectronic Mixers with Optimized Conversion Efficiency

Jae-Young Kim, Myung-Jae Lee and Woo-Young Choi

Department of Electrical Electronic Engineering

Yonsei University

Seoul, Korea

wchoi@yonsei.ac.kr

Abstract—A harmonic optoelectronic mixer based on CMOS avalanche photodiode is designed for optimized conversion efficiency in 60-GHz band. By reducing P-N junction capacitance in the avalanche photo-detection region and parasitic n-well/substrate capacitance, the supplied 30-GHz LO is efficiently converted to the 60-GHz harmonic LO signal and generates up-converted RF signals from optical IF. In addition, the silicide layer under the metal contact reduces the parasitic resistance and enhances the mixer conversion efficiency.

I. INTRODUCTION

There are growing research interests for millimeter-wave wireless systems. In particular, the 60-GHz band is very attractive for short range high-speed wireless networks such as wireless personal area network (WPAN) and wireless local area network (WLAN) due to the wide bandwidth of about 7-GHz it can provide. However, the wireless coverage of the millimeter-wave communication is limited to a few meters due to the large transmission loss in the air. Consequently, a large number of antenna base stations and effective distribution networks are required for implementation of WLAN in the millimeter-wave band.

The fiber-fed millimeter-wave wireless system is an attractive technology that can simplify the antenna base stations and reduce the overall cost [1-3]. Especially, the remote up-conversion scheme can reduce the burden of high-speed optical component [3]. In this system, broadband data signals are optically distributed from central station to antenna base stations via optical fiber, and then frequency converted to millimeter-wave band in antenna base station for transmission to mobile terminals through wireless link. In this scheme, optoelectronic mixer (O/E mixer) is the key device in antenna base station with multi-functionality of photo-detection and frequency conversion of optical IF to RF signals [4-7].

The several types of O/E mixer have been reported that are based on InP high-electron mobility transistor [4], InP heterojunction bipolar transistor (HBT) [5], or CMOS

compatible avalanche photodiode (CMOS-APD) [6-7]. The InP-based O/E mixers offer good photo-detection and frequency conversion efficiencies which allow utilization of the optically distributed local oscillator (LO) from central station in great simplification of antenna base stations [5]. However, InP technologies are not cost effective for wide commercial applications as of yet. In contrast, optoelectronic mixers based on CMOS technology has the capacity for integration of optoelectronic devices with powerful CMOS circuits. In addition, CMOS-based photo-detectors can detect 850nm light, allowing the use of multi-mode fiber (MMF) and a vertical-cavity surface-emitting laser (VCSEL), which can further enhance the system cost effectiveness.

However, CMOS-APD O/E mixers have relatively poor photo-detection and frequency conversion efficiency compared to InP-based O/E mixer, which directly affects on the optical sensitivity of the antenna base station. In order to reduce this problem, we performed optimization for conversion efficiency for CMOS-APD 60-GHz band harmonic O/E mixers and the results are presented in this paper.

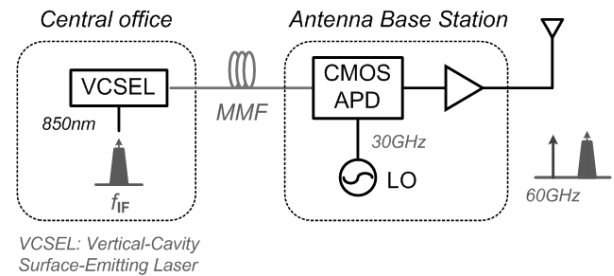


Figure 1. Schematic diagram of fiber-fed 60-GHz wireless system based on CMOS APD O/E mixer

I. OPERATION PRINCIPLE OF CMOS APD O/E MIXER

Fig. 1 shows the schematic of fiber-fed 60-GHz wireless system based on CMOS-APD O/E mixer. In this system,

optical IF signals are generated in the central station using low-cost VCSEL and transmitted to the antenna base station through MMF. In the antenna base station, the optical IF signals are photo-detected and harmonically frequency up-converted to 60-GHz band by CMOS-APD O/E mixer using 30-GHz LO. Then frequency up-converted RF signals are radiated to mobile terminals through the wireless channel.

The cross-section of a CMOS-APD O/E mixer fabricated with $0.13\mu\text{m}$ standard CMOS process is shown in Fig. 2. Vertically injected optical IF signals are photo-detected by the vertical P-N junction between P+ and N-well regions [8]. The resulting photo-currents are collected by multi-finger electrodes on P+ region so that slow diffusion currents generated in the N-well/P-substrate junction are blocked. ADPs having two different lateral dimensions, $10\times 10\mu\text{m}^2$ and $30\times 30\mu\text{m}^2$, are characterized.

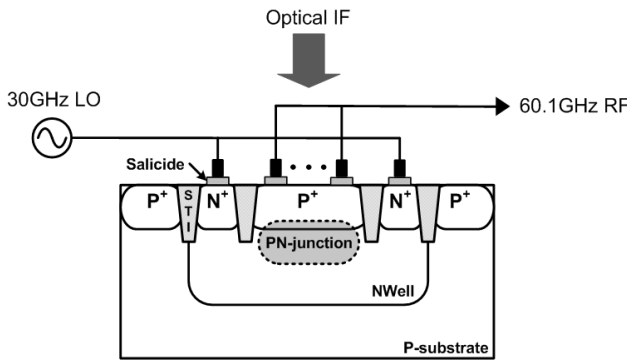


Figure 2. Cross-sectional structure of CMOS APD and O/E mixer configuration

II. PHOTO-DETECTION CHARACTERISTICS

Fig. 3 shows dc photo-currents of the fabricated CMOS-APDs with different active areas of $10\times 10\mu\text{m}^2$ and $30\times 30\mu\text{m}^2$, when optical power of 0dBm is injected through lensed fiber of 10um spot diameter. The optical responsivity strongly depends on the reverse bias voltage because the avalanche multiplication gain is determined by the electric field applied to the P-N junction [8]. The measured optical responsivities of $10\times 10\mu\text{m}^2$ and $30\times 30\mu\text{m}^2$ devices are comparable. This means that both of the photo-detection efficiency and avalanche gain are not significantly affected by the device size. The peak avalanche gain for $10\times 10\mu\text{m}^2$ and $30\times 30\mu\text{m}^2$ devices are 112 and 121, respectively, at reverse bias voltage of 10.3V.

Fig. 4 shows the photo-detection frequency response measured at reverse bias voltage of 10.25V where the response is largest. The incident optical power is 0dBm. As can be seen, $10\times 10\mu\text{m}^2$ APD has much larger bandwidth ($\text{BW}_{-3\text{dB}}=5.75\text{GHz}$) than $30\times 30\mu\text{m}^2$ APD ($\text{BW}_{-3\text{dB}}=2.1\text{GHz}$). It's mainly due to the reduced RC time constant of the smaller device with smaller junction capacitance.

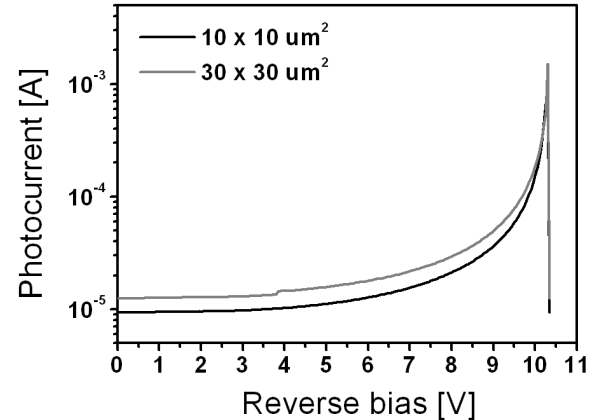


Figure 3. DC photo-current of the CMOS APD as a function of reverse bias voltage applied in N-well. Incident optical power is 0dBm

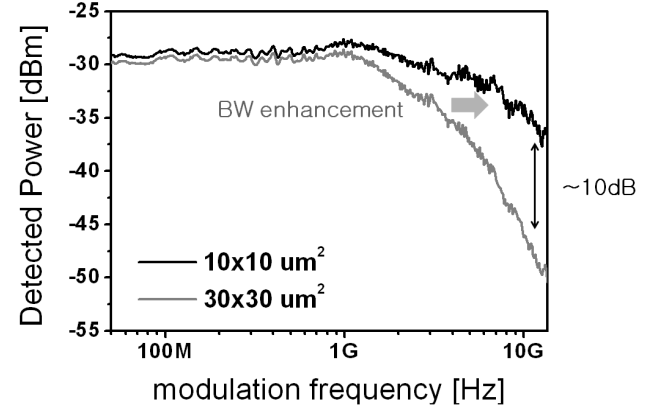


Figure 4. Photo-detection frequency response of CMOS APD at reverse bias voltage of 10.25V and incident optical power of 0dBm

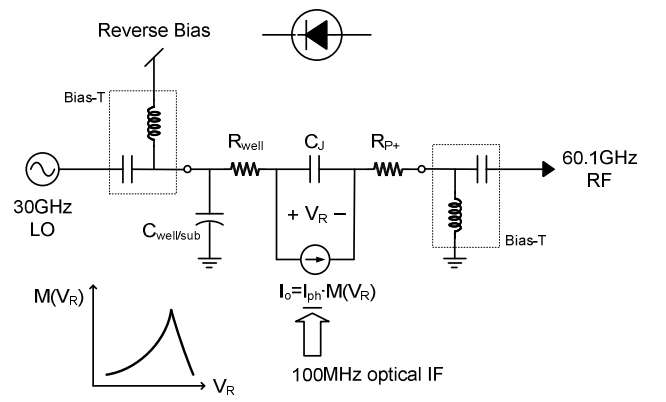


Figure 5. Equivalent circuit model description of CMOS APD-based harmonic O/E mixer

III. CONVERSION EFFICIENCY OPTIMIZATION

For O/E mixing operation, 30-GHz LO is applied to N-well of the APD as shown in Fig. 2, which modulates the input optical IF signals to generates 60-GHz RF signals. The detailed operation is described in Fig. 5 with an equivalent circuit model for the APD. In this model, the output photocurrent of APD is a product of the primarily photo-detected current of optical IF (I_{ph}) and the avalanche multiplication gain (M) which is a function of the reverse bias voltage across the P-N junction (V_R). So, when 30-GHz LO signals are applied to the APD, the nonlinearity of multiplication gain for V_R generates 2nd order harmonic LO in 60-GHz and also RF signals in 60.1-GHz by modulation of the 100-MHz optical IF signals.

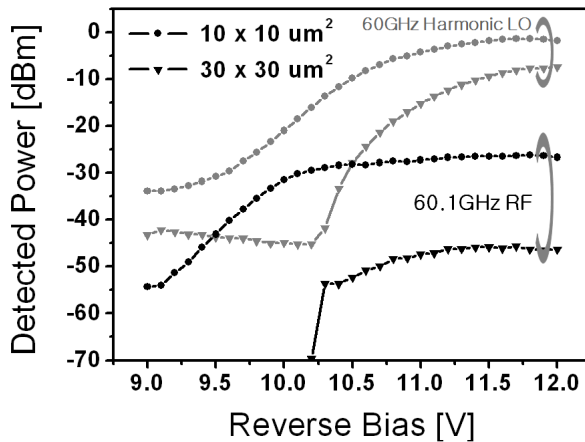


Figure 6. Measured power of 60-GHz harmonic LO and 60.1-GHz frequency up-converted RF signal when the APD size is $10 \times 10 \mu\text{m}^2$ and $30 \times 30 \mu\text{m}^2$ separately. The incident optical power is 0dBm.

In high frequencies such as 30-GHz, however, the junction capacitance (C_J) exhibits very low impedance which is inversely proportional to frequency. Consequently, a large portion of the supplied LO power passes the P-N junction through the junction capacitance and only a small portion of the supplied LO remains as the voltage swing across the intrinsic P-N junction (V_R) resulting in conversion efficiency degradation. In addition, the parasitic capacitance between N-well and P-substrate ($C_{well/sub}$) causes power loss of the high frequency LO. These losses of LO by junction capacitance and parasitic capacitance can be easily improved by reducing the lateral size of the APD. Fig. 6 shows the measured powers of 60-GHz harmonic LO and 60.1-GHz frequency up-converted signals from the APDs of different size. The $10 \times 10 \mu\text{m}^2$ APD has minimum 20 dB larger conversion efficiency than the $30 \times 30 \mu\text{m}^2$ device.

The parasitic resistances such as N-well resistance or P+ contact resistance also can degrade the O/E mixing efficiency. Fig. 7 shows comparison of conversion efficiencies between $10 \times 10 \mu\text{m}^2$ APDs for which P+ contacts are formed with and without the silicided layer. The silicided layer reduces P+

contact resistance from few ohms to nearly zero. Even though the silicided layer does not affect the photo-detection characteristics, for O/E mixing operation, the APD with silicided layer has from 7 to 17dB larger conversion efficiency than the one without silicided layer.

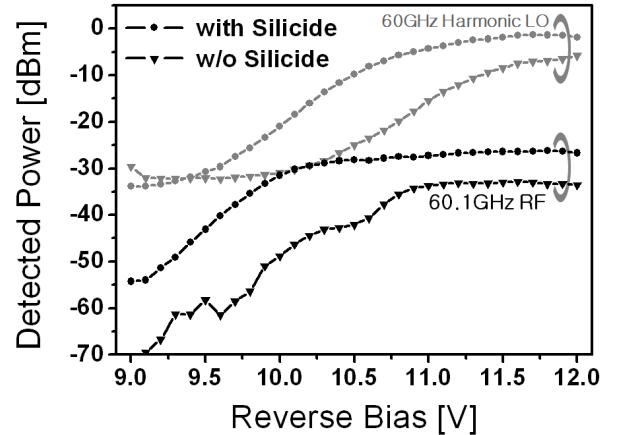


Figure 7. Measured power of 60-GHz harmonic LO and 60.1-GHz frequency up-converted RF signal when P⁺ contact of the APD is formed with and without salicidized layer. The APD size is $10 \times 10 \mu\text{m}^2$ and the incident optical power is 0dBm.

IV. CONCLUSION

The CMOS-APD 60-GHz harmonic optoelectronic mixers are investigated for conversion efficiency enhancement. By reducing the junction capacitance and parasitic losses, the 2nd order LO and frequency up-converted signal power can be significantly improved. In addition, down-sizing of the APD can improve the photo-detection bandwidth for optical IF detection maintaining the optical responsivity. The resulting frequency conversion loss of the optimized 60-GHz O/E mixer is about 1.5dB.

ACKNOWLEDGMENT

This work was supported by the Seoul Development Institute under the Seoul R&BD Program (NT080542). The chip was fabricated through the MPW of IC Design Education Center (IDEC) supported by the Korea Ministry of Knowledge Economy (MKE).

REFERENCES

- [1] A. J. Seeds, "Microwave photonics," IEEE Trans. Microw. Theory Tech., vol. 50, no. 3, pp. 877-887, March 2002.
- [2] G. H. Smith and D. Novak, "Broadband millimeter-wave fiber-radio network incorporating remote up-down conversion," IEEE MTT-S Int. Microw. Symp. Dig., Baltimore, MD, pp. 1509-1512, June 1998.
- [3] H. Ogawa, D. Polifko and S. Banba, "Millimeter-wave fiber optics systems for personal radio communication," IEEE Trans. Microw. Theory Tech., vol. 40, no. 12, pp. 2285-2293, December 1992.
- [4] C. S. Choi, H. S. Kang, W. Y. Choi, D. H. Kim, and K. S. Seo, Phototransistors based on InP HEMTs and their applications to millimeter-wave radio-on-fiber systems," IEEE Trans. Microw. Theory Tech., Vol. 53, No. 1, pp.256-263, January 2005.

- [5] C. S. Choi, J. H. Seo, W. Y. Choi, H. Kamitsuna, M. Ida, and K. Kurishima, “60-GHz bidirectional radio-on-fiber links based on InP-InGaAs HPT optoelectronic mixers,” *IEEE Photon. Technol. Lett.*, vol. 17, no. 12, pp. 2721–2723, December 2005.
- [6] H. S. Kang and W. Y. Choi, “CMOS-compatible 60 GHz harmonic optoelectronic mixer,” *IEEE MTT-S Int. Microw. Symp. Dig.*, pp. 233–236, June 2007.
- [7] M. J. Lee, H. S. Kang, K. H. Lee and W. Y. Choi, “Self-Oscillating Harmonic Opto-Electronic Mixer Based on a CMOS-Compatible Avalanche Photodetector for Fiber-Fed 60-GHz Self-Heterodyne Systems,” *IEEE Trans. Microw. Theory Tech*, vol. 56, no. 12, pp.3180-3187, December 2008.
- [8] H. S. Kang, M. J. Lee and W. Y. Choi, “Si avalanche photodetectors fabricated in standard complementary metal-oxide-semiconductor process,” *Applied Physics Lett.*, vol. 90, 151118, April 2007